ENTERED 106121

New Mexico Geological Society Guidebook, 58th Field Conference, Geology of the Jemez Mountains Region II, 2007, p. 284-295.

PLIOCENE VOLCANIC ROCKS OF THE TSCHICOMA FORMATION, EAST-CENTRAL JEMEZ VOLCANIC FIELD: CHEMISTRY, PETROGRAPHY, AND AGE CONSTRAINTS

DAVID BROXTON[1], GIDAY WOLDEGABRIEL[1], LISA PETERS[2], JAMES BUDAHN[3], AND GARY LUEDEMANN[1]
[1] Los Alamos National Laboratory, Mail Stop T003, P.O. Box 1663, Los Alamos, NM 87544, broxton@lanl.gov
[2] New Mexico Bureau of Geology and Mineral Resources; New Mexico Institute of Mining and Technology, 801 Leroy Place, Socorro, NM 87801
[3] U.S. Geological Survey, P.O. Box 25046, Federal Center, Mail Stop 974, Lakewood, CO 80225

ABSTRACT — The Tschicoma Formation in the central and southern Sierra de los Valles is composed of thick sequences of silicic to intermediate lavas and subordinate tuffs that erupted from overlapping dome and flow complexes over a period of about 2.5 m.y. during the Pliocene. The chemical and petrographic characteristics of the individual dome complexes are discussed in detail, and are sufficiently distinct that the lavas can be readily distinguished from one another. A south to north description of the dome complexes is as follows. The Dacite of Sawyer Dome contains 32-34% phenocrysts of plagioclase, hornblende, and orthopyroxene, and two $^{40}Ar/^{39}Ar$ ages range from 3.18 to 3.67 Ma. The Dacite of Cerro Grande contains about 21% phenocrysts of plagioclase, hornblende, orthopyroxene, and subordinate clinopyroxene; three $^{40}Ar/^{39}Ar$ ages range from 2.88 to 3.35 Ma. The Dacite of Pajarito Mountain is divided into a lower and upper series of lavas. The lower series is a two-pyroxene dacite characterized by 10.3-16.4% phenocrysts of plagioclase and subequal orthopyroxene and clinopyroxene, whereas the upper series contains 23-24% phenocrysts of plagioclase, orthopyroxene, and subordinate clinopyroxene, and the lava chemistry is slightly more silicic. Two samples from the upper series lavas produced $^{40}Ar/^{39}Ar$ ages of 2.93 and 3.09 Ma. The Rhyodacite of Rendija Canyon contains 11-16% phenocrysts consisting of quartz and plagioclase, subordinate sanidine and anorthoclase, and low (<0.5%) amounts of biotite ± clinopyroxene ± hornblende. It is predominantly a low-silica rhyolite with $^{40}Ar/^{39}Ar$ ages of 4.98 and 5.04 Ma. A sample of high-silica rhyolite from a small ash-flow tuff near the base of the sequence yielded an $^{40}Ar/^{39}Ar$ age of 5.36 Ma. The Dacite of Caballo Mountain consists of two main parts. The summit area of Caballo Mountain is underlain by dacite containing about 2% phenocrysts consisting of subequal plagioclase and hornblende, subordinate clinopyroxene, and trace quartz and orthopyroxene. These relatively crystal-poor lavas overlie lavas that contain up to 24% phenocrysts consisting of plagioclase, hornblende, subordinate quartz and biotite, and minor to trace sanidine, orthopyroxene, and clinopyroxene. The crystal-poor summit dacite yielded an $^{40}Ar/^{39}Ar$ age of 3.06 Ma and the crystal-rich dacite returned an $^{40}Ar/^{39}Ar$ age of 4.66 Ma. After about 2.88 Ma, Tschicoma volcanism in the Sierra de los Valles died out and intermediate volcanism shifted eastwards to the western Española basin where several small-volume dacite lavas erupted between 2.36 and 2.74 Ma.

INTRODUCTION

Porphyritc dacitic lavas of the Tschicoma Formation of the Polvadera Group erupted primarily as large, overlapping flow and dome complexes typified by the extensive exposures of this formation in the highlands of the Sierra de los Valles west of the Pajarito fault zone (Fig. 1). Previously published ages for lavas of the Tschicoma Formation range from 2.96 ± 0.27 to 6.9 ± 0.2 Ma (Dalrymple et al., 1967; Luedke and Smith, 1978; Gardner et al., 1986; Goff and Gardner, 2004), but the main volume of volcanic rocks apparently erupted between 3 and 5 Ma (Goff and Gardner, 2004). Smith (1938) first mapped these rocks as the Chicoma volcanic formation in the Abiquiu quadrangle, presumably naming them for the high peak composed of these rocks called Tschicoma Mountain on modern topographic maps (Griggs, 1964). Griggs renamed these rocks the Tschicoma Formation and identified two mappable units: an older unit composed of latite and quartz latite and a younger unit composed of pyroxene andesite. The quartz latite of the older unit is equivalent to the Rhyodacite of Rendija Canyon of this paper and the latite encompasses the dacites of Sawyer Dome, Cerro Grande, Pajarito Mountain, and Caballo Mountain. The younger pyroxene andesite was mapped in a small area north of Quemazon Canyon and is probably correlative with the phenocryst-poor (<5%) dacite exposed along Pipeline Road that yielded a Cerro Toledo Rhyolite age (1.50 ± 0.13 Ma), as described in this paper.

Bailey et al. (1969) placed the Tschicoma Formation within the Polvadera Group that includes, from oldest to youngest, the Lobato Basalt, Tschicoma Formation, and El Rechuelos Rhyolite. The Polvadera Group was believed to be younger than the Keres Group and overlapped it to the south (see Goff and Gardner, 2004 for further discussion). Smith et al. (1970) showed the Tschicoma Formation as an undivided unit that is widely distributed throughout the eastern and northern part of the Jemez Mountains on their geologic map of the Jemez volcanic field. Additional Tschicoma Formation almost certainly foundered into the Valles caldera where it is now buried by Bandelier Tuff and post-Bandelier caldera fill.

The individual lavas making up the Tschicoma Formation in the central and southern Sierra de los Valles and their source dome complexes were first described as part of a field guidebook for the Jemez volcanic field (Goff et al., 1989, Day 2, Stop 4). These descriptions included summaries of the chemical and petrographic characteristics for each of the major dome complexes. The STATEMAP program is currently mapping the geology of the Jemez volcanic field at a scale of 1:24,000. Preliminary geologic maps for the Guaje Mountain (Kempter and Kelley, 2002), Bland (Goff et al., 2005), and Valle Toledo (Gardner et al, 2006) 7.5-minute quadrangles are now available. These maps and their accompanying text describe the distribution of units of the Tschicoma Formation discussed in this paper and provide information

31754

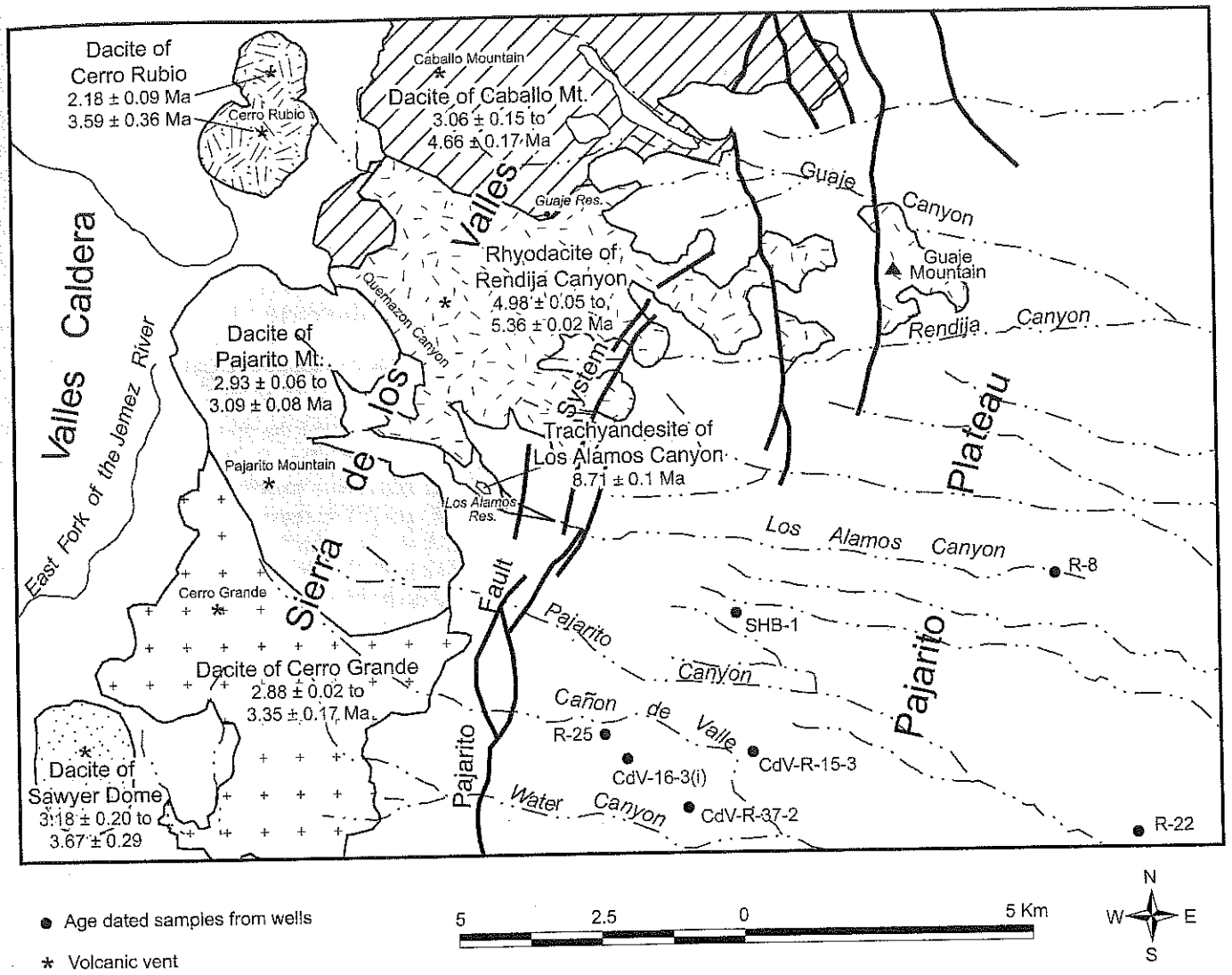

FIGURE 1. Location map showing the distribution of the major Tschicoma volcanic centers in the central and southern Sierra de los Valles. Age dates are from this paper except for those for Cerro Rubio (from Heiken et al., 1986).

about their field relationships, outcrop characteristics, and ages. The names for geologic units used in this paper are the same as those used on these maps.

This paper also presents information relevant to understanding the depositional history of the Pliocene Puye Formation. The Puye Formation is a large apron of overlapping alluvial and pyroclastic fans shed eastward from the Jemez volcanic field into the western Española basin (Smith, 1938; Griggs, 1964; Bailey et al., 1969; Turbeville et al., 1989; Waresback and Turbeville, 1990). Because its primary source area was volcanic domes in the Sierra de los Valles, the Puye Formation overlaps and postdates the Tschicoma Formation in age. Turbeville et al. (1989) estimated its areal distribution at 518 km^2 and its volume at ~15 km^3. The formation reaches a maximum thickness of >330 m in well R-25 on the western side of the Pajarito Plateau (Broxton et al., 2002). Its thickness in the central and eastern parts of the plateau is ~200 m where the upper part contains interbedded basaltic lavas of the Cerros del Rio volcanic field.

This paper describes the chemistry, petrography, mineral chemistry, and ages of eruptive centers of the Tschicoma Formation in the central and southern Sierra de los Valles between Sawyer Dome on the south and Caballo Mountain on the north (Fig. 1). The centers of Tschicoma Mountain, Polvadera Peak, and others in the northern Jemez Mountains are not discussed here. The data presented contribute to understanding the spatial and temporal trends in volcanism and tectonism in the Jemez volcanic field during the Pliocene, and they provide information about the timing, composition, and distribution of source areas that provided detritus to the Puye Formation. Ages and their supporting analytical data are also presented for tephras interbedded within the Puye Formation; these tephras are useful time-stratigraphic markers for understanding the internal structure and sediment accumulation rates for these fan deposits. Finally, ages are presented for small-volume dacites erupted in the western part of the Española basin to determine their temporal relationship to the Tschicoma Formation.

METHODS

Samples of Tschicoma lavas and tuffs were collected from outcrops in the Sierra de los Valles. Vitrophyres of lavas were sampled where possible, but most samples represent devitrified lava interiors. Vitric tuffs were sampled in Guaje Canyon. Pliocene lavas and tephras from the Pajarito Plateau were sampled from borehole core and cuttings.

Major and trace elements for 38 samples were analyzed using an automated Rigaku wavelength-dispersive X-ray fluorescence (XRF) spectrometer. Samples were first crushed and homogenized in 5-10 g portions in a tungsten-carbide ballmill. Sample splits were heated at 110°C for 4 hrs, and then allowed to equilibrate at ambient laboratory conditions for 12 hrs. To obtain fusion disks, one-gram splits were mixed with 9 g of lithium tetraborate flux and heated in a muffle furnace for 45 minutes at 1100°C. Elemental concentrations were calculated by comparing X-ray intensities for the samples to those for standard BCR-1. Intensities were reduced using a fundamental parameters program for matrix corrections software by Criss (1979).

The abundances of 33 major, minor and trace elements, including 11 rare-earth elements (REE), were determined on the samples by instrumental neutron activation analysis (INAA). About 1.0 g samples were irradiated in the USGS-TRIGA reactor at a flux of 2.5×10^{12} n/cm^2/sec for eight hours. Three sequential counts at 7 days, 14 days, and 65 days after the irradiation were made on both coaxial and planar germanium detectors. A summary of the INAA procedure used at the USGS is given in Budahn and Wandless (2002). Precision and accuracy for most of the elements determined (including La, Yb, Hf, Rb, Th, and U) range from 1 to 5%. Only five elements have precision errors of greater than 10% (including Ho, Tm, and Sb) based on counting statistic errors. Accuracy is based on replicate analysis of USGS standard reference materials, including BHVO-1. Because of their high precision and overlap with XRF trace elements, only the more extensive NAA trace element data are used in this paper.

Phenocryst compositions were determined using a Cameca SX50 electron microprobe, equipped with four wavelength dispersive spectrometers (WDS). Quantitative WDS analyses were obtained at 15 kV accelerating voltage and 15 nA beam current. All analyses were obtained with a 5 μm beam diameter. Calibrations of all analyzed elements at the same analytical conditions were carried out on natural and glass standards.

Phenocryst volume percentages were primarily determined by standard modal point counts. For lavas of Caballo Mountain, the makeup of the phenocryst population was first determined using standard transmitted- and reflected-light petrographic techniques. Then, thin sections were captured as digital images on a high-resolution scanner, and felsic and mafic phenocryst abundances were determined by image analysis performed on a computer using the public domain NIH Image program (developed at the U.S. National Institutes of Health and available on the internet at: <http://rsb.info.nih.gov/nih-image/> . Abundances of individual felsic and mafic phases were determined by tallying the areas of subordinate phenocryst types and then subtracting their area from the felsic or mafic totals. A comparison of mineral abundances by standard point counts and image analysis agreed within 10%.

Selected samples were dated by the $^{40}Ar/^{39}Ar$ method at the New Mexico Geochronology Laboratory in Socorro. Sample preparation and irradiation, instrumentation, and analytical parameters are described in Table 1. Procedures for gas extraction and mass spectrometer follow those outlined in McIntosh and Cather (1994). Step heating and isochron diagrams are available in Broxton et al. (2007).

RESULTS

In this section we describe chemical, petrographic, and age characteristics of the Tschicoma lavas in the Sierra de los Valles. Unit descriptions are organized around the principal eruptive centers, described from south to north (Fig. 1). Representative chemical analyses (Table 2) are recast on a volatile-free basis in the following sections. Table 3 presents representative petrographic data for these rocks, and Table 4 relates the $^{40}Ar/^{39}Ar$ results to lavas of the Tschicoma Formation in the Sierra de los Valles and to subsurface Pliocene tephras and dacite lavas of the Pajarito Plateau. Complete chemical, microprobe, petrographic, and $^{40}Ar/^{39}Ar$ data for all samples collected as part of this study are available upon request from the lead author and most can be accessed in the database of Warren et al. (2005). We present an alkali-silica plot showing the classification of rock types (Fig. 2), bivariate plots comparing selected major and trace elements (Fig. 3), and chondrite-normalized plots of rare-earth elements (Fig. 4). A single analysis of the Dacite of Cerro Rubio (in Figs. 3, 4) is included for comparison to rocks described in this paper. Cerro Rubio is a dome and intrusive complex of the Tschicoma Formation located west of Caballo Mountain (Fig.1) that is described by Griggs (1964) and Goff and Gardner (2004).

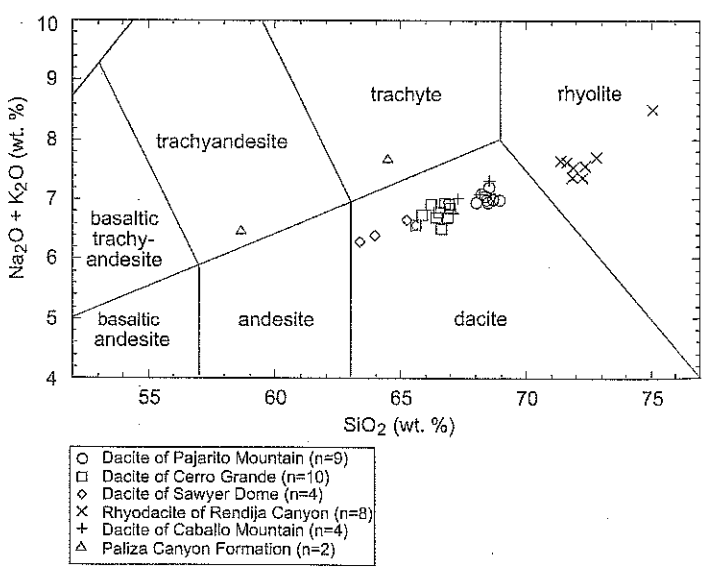

FIGURE 2. Alkali-silica diagram for samples of Tschicoma Formation from the Sierra de los Valles. Samples of trachyandesite and trachyte are part of the Paliza Canyon Formation. Rock classifications follow the IUGS usage of Le Bas et al. (1986). Analyses are plotted on a volatile-free basis.

TABLE 1. Analytical Methods for $^{40}Ar/^{39}Ar$ dates. See Table 4 for ages.

Sample	Lab #	Irradiation	Mineral	Age Analysis	# of crystals/steps
SHB-1-656	520	nmum-6	groundmass concentrate	furnace step-heat	3
SHB-1-694	532	nmum-6	groundmass concentrate	furnace step-heat	3
6-22-83-9	51441	NM-127	groundmass concentrate	furnace step-heat	10
6-22-83-12	51443	NM-127	groundmass concentrate	furnace step-heat	5
10-8-90-2a	51445	NM-127	groundmass concentrate	furnace step-heat	7
6-22-83-3	51509	NM-127	groundmass concentrate	furnace step-heat	5
6-22-83-5	51445	NM-127	hornblende	furnace step-heat	7
10-8-90-4	51457	NM-127	hornblende	furnace step-heat	8
8-21-88-1	51454	NM-127	groundmass concentrate	furnace step-heat	10
7-1-83-1	51442	NM-127	groundmass concentrate	furnace step-heat	9
R-22 628-638	52725	NM-144	groundmass concentrate	furnace step-heat	6
CDV-R-15-3 992-997	52727	NM-144	groundmass concentrate	furnace step-heat	5
5-25-83-1	52692	NM-144	hornblende	furnace step-heat	8
5-25-83-2	55193	NM-182	hornblende	furnace step-heat	7
CDV-16-3(i) 1380-1385	55182	NM-182	groundmass concentrate	furnace step-heat	3
R-8 95-95.1	55180	NM-182	groundmass concentrate	furnace step-heat	10
11-19-84-1	52642	NM-144	sanidine	laser total fusion	5
R-25 1922-1923	55188	NM-182	sanidine	laser total fusion	10
LAPC98-13	52644	NM-144	sanidine	laser total fusion	14
DEB 10-91-7	51452	NM-127	sanidine	laser total fusion	15

Sample preparation and irradiation:

Mineral separates were prepared using standard crushing, dilute acid treatment, heavy liquid and hand-picking techniques. Separates from nmum-6 were loaded into a machined Al discs and irradiated for 1 hour in the L-67 position, Ford Memorial Reactor, University of Michigan, Ann Arbor, MI. Separates from NM-127 were loaded into a machined Al disc and irradiated for 14 hours in the D-3 position, Nuclear Science Center, College Station, TX. Separates from NM-144 and NM-154 were loaded into a machined Al disc and irradiated for 7 hours in the D-3 position, Nuclear Science Center, College Station, TX. Separates from NM-182 were loaded into a machined Al disc and irradiated for 10 hours in the D-3 position, Nuclear Science Center, College Station, TX. NM-182 values $(^{40}Ar/^{39}Ar)_K = 0.0\pm0.0004$; $(^{36}Ar/^{37}Ar)_{Ca} = 0.00028\pm0.00001$; and $(^{39}Ar/^{37}Ar)_{Ca} = 0.0007\pm0.00002$.

Neutron flux monitor Fish Canyon Tuff sanidine (FC-1). Assigned age = 28.02 Ma (Renne et al, 1998) relative to Mmhb-1 at 520.4 Ma (Samson and Alexander, 1987).

Instrumentation:

Mass Analyzer Products 215-50 mass spectrometer on line with automated all-metal extraction system.

Furnace analyses were step-heated for 8-14 minutes using a Mo double-vacuum resistance furnace.

Reactive gases removed during furnace analysis by reaction with 3 SAES GP-50 getters, 2 operated at ~450°C and 1 at 20°C. Gas also exposed to a W filament operated at ~2000°C.

Single crystal sanidine were fused by a 50 watt Synrad CO2 laser.

Reactive gases removed during a 2 minutes reaction with 2 SAES GP-50 getters, one operated at ~450°C and one at 20°C. Gas also exposed to a W filament operated at ~2000°C and a cold finger operated at -140°C.

Analytical parameters:

6.0×10^{-17} moles/pA for nmum-6, 1.46×10^{-16} moles /pA for NM-127, 2.89×10^{-16} moles/pA for NM-144, 2.36×10^{-16} moles/pA for NM-154, 1.89×10^{-16} moles/pA for NM-182.

Electron multiplier sensitivities for the laser analyses are as follows:

44×10^{-16} moles/pA for NM-127, 1.85x 10-16 moles/pA for NM-144.

Total system blank and background averaged 1040, 6.6, 1.6, 16.9, 5.5×10^{-18} moles at masses 40, 39, 38, 37 and 36, respectively for the furnace analyses. Total system blank and background averaged 124, 1.4, 0.2, 1.1, 0.7×10^{-18} moles at masses 40, 39, 38, 37 and 36, respectively for the laser analyses.

J-factors determined to a precision of ± 0.1% by CO_2 laser-fusion of 4 single crystals from each of 4 or 6 radial positions around the irradiation tray.

Correction factors for interfering nuclear reactions were determined using K-glass and CaF_2 and are as follows:

NM-6 values $(^{40}Ar/^{39}Ar)_K = 0.00020\pm0.0003$; $(^{36}Ar/^{37}Ar)_{Ca} = 0.00026\pm0.00002$; and $(^{39}Ar/^{37}Ar)_{Ca} = 0.00070\pm0.00005$, NM-127 values $(^{40}Ar/^{39}Ar)_K = 0.00020\pm0.0003$; $(^{36}Ar/^{37}Ar)_{Ca} = 0.00026\pm0.00002$; and $(^{39}Ar/^{37}Ar)_{Ca} = 0.00070\pm0.00005$, NM-144 values $(^{40}Ar/^{39}Ar)_K = 0.00020\pm0.0003$; $(^{36}Ar/^{37}Ar)_{Ca} = 0.00028\pm0.000005$; and $(^{39}Ar/^{37}Ar)_{Ca} = 0.0007\pm0.00002$, NM-154 values $(^{40}Ar/^{39}Ar)_K = 0.0002\pm0.0003$; $(^{36}Ar/^{37}Ar)_{Ca} = 0.00028\pm0.000005$; and $(^{39}Ar/^{37}Ar)_{Ca} = 0.0007\pm0.00002$, NM-182 values $(^{40}Ar/^{39}Ar)_K = 0.0\pm0.0004$; $(^{36}Ar/^{37}Ar)_{Ca} = 0.00028\pm0.00001$; and $(^{39}Ar/^{37}Ar)_{Ca} = 0.0007\pm0.00002$.

UNITS

Dacite of Sawyer Dome

The Dacite of Sawyer Dome is a thick stack of coarsely phyric lavas that is composed of medium-K hornblende dacite (Figs. 2, 3). On a volatile-free basis, these lavas are low in SiO_2 (63.4 to 65.6%) and high in TiO_2 (0.65-0.70%), Fe_2O_3T (4.78-4.98%), and Sr (654-711 ppm) compared to most other lavas of the Tschicoma Formation described in this paper (Fig. 3; Table 2). Stratigraphically higher rocks near the top of Sawyer Dome are more silicic than those near the base, suggesting a trend towards slightly more silicic compositions over time. Chondrite-normalized rare-earth element patterns overlap those of the other dacites and they lack a negative Eu anomaly (Fig. 4).

TABLE 2. Representative chemical analyses for lavas of the Tschicoma Formation in the Sierra de los Valles.

	Dacite of Sawyer Dome			Dacite of Cerro Grande			Dacite of Pajarito Mountain			Rhyodacite of Rendija Canyon			Dacite of Caballo Mountain		
Sample Number	5-25-83-1	5-25-83-2	5-25-83-4	6-22-83-3	6-22-83-4	6-22-83-6	5-5-83-1	6-22-83-7	6-22-83-9	11-19 84-3	1-1-85-2	7-8-83-2	8-21-88-1	7-5-85-1	7-5-85-3
Notes							lower series	upper series	upper series				upper xtal poor	lower xtal rich	lower xtal rich
XRF Major Elements (wt. %)															
SiO_2	62.2	63.2	64.4	65.8	65.9	65.9	66.1	68.5	68.9	70.7	69.7	70.7	65.7	66.3	66.2
TiO_2	0.69	0.68	0.64	0.57	0.57	0.57	0.57	0.47	0.48	0.33	0.38	0.31	0.55	0.49	0.55
Al_2O_3	17.0	16.8	15.9	15.4	15.6	15.9	15.0	15.2	15.5	13.7	14.0	13.8	15.8	14.6	14.8
Fe_2O_3T	4.89	4.72	4.72	4.32	4.40	4.32	4.15	3.39	3.75	2.54	2.95	2.83	3.89	3.40	4.23
MnO	0.08	0.09	0.06	0.07	0.09	0.08	0.08	0.06	0.06	0.05	0.05	0.06	0.06	0.06	0.07
MgO	2.2	2.14	1.99	2.02	1.81	2.12	1.95	1.43	1.36	1.43	0.59	1.47	1.70	1.76	1.87
CaO	4.72	4.6	4.19	3.85	3.42	4.17	3.90	3.18	3.15	2.31	2.20	2.23	3.43	3.54	3.48
Na_2O	3.78	4.08	3.99	4.05	3.88	4.22	3.99	3.81	3.89	3.44	3.59	3.78	3.69	3.71	3.33
K_2O	2.39	2.23	2.57	2.65	2.71	2.53	3.04	3.15	3.13	3.81	3.83	3.80	2.91	3.19	3.59
P_2O_5	0.25	0.24	0.25	0.22	0.2	0.22	0.29	0.17	0.16	0.08	0.10	0.10	0.24	0.23	0.26
Total	98.2	98.8	98.7	98.9	98.6	100.0	99.1	99.4	100.4	98.4	97.4	99.1	98.0	97.3	98.4
NAA Trace Elements (ppm)															
Rb	37.7		39.5		43.1	33.8	51	63.6	62.2	107	105	124	45.5	58.2	69.8
Sr	711		654		499	609	613	446	441	313	293	337	612	553	566
Cs	0.765		0.477		0.351	0.431	1.26	0.521	0.728	15.5	2.17	5.4	0.435	1.4	2.23
Ba	1130		1230		1410	1270	1190	1360	1380	890	889	654	1330	1220	1080
Th	5.96		5.71		4.81	4.78	8.05	6.06	4.85	14.9	14	20.7	7.53	7.98	12
U	1.54		1.69		1.39	1.34	2.48	1.61	1.3	5.24	4.76	6.75	2.22	2.55	4.19
La	39.4		38.8		38.1	37.5	41	38.6	38.1	35.6	41.6	36	35.2	39.6	49.3
Ce	67.5		67.9		69.6	66.1	72.2	70.2	66.4	61.8	75.3	61.1	60.1	70.3	76.7
Nd	26.1		27		28.5	27.3	28.2	28.1	28.7	20.6	24.5	19.7	24.3	27.4	31
Sm	5.03		4.95		5.1	4.91	4.73	5.26	5.27	4.02	4.2	4	4.31	4.92	5.53
Eu	1.35		1.32		1.3	1.27	1.25	1.18	1.15	0.706	0.793	0.625	1.1	1.17	1.21
Gd	3.95		4.23		3.95	3.67	4.08	3.8	4.01	3.35	3.38	3.8	3.49	3.94	4.09
Tb	0.54		0.526		0.557	0.531	0.497	0.519	0.529	0.442	0.464	0.503	0.43	0.488	0.574
Ho	0.685		0.69		0.662	0.66	0.629	0.657	0.651	0.647	0.614	0.787	0.545	0.656	0.737
Tm	0.256		0.271		0.274	0.254	0.245	0.249	0.245	0.297	0.265	0.377	0.204	0.242	0.299
Yb	1.58		1.68		1.65	1.56	1.46	1.48	1.5	1.9	1.66	2.39	1.24	1.52	1.79
Lu	0.224		0.235		0.242	0.222	0.206	0.212	0.214	0.278	0.239	0.352	0.179	0.218	0.259
Zr	166		171		172	173	160	184	172	142	143	129	149	169	172
Hf	4.53		4.35		4.66	4.51	4.14	4.78	4.71	4.02	4.32	3.98	3.93	4.28	4.22
Sc	9.36		9.1		8.4	8.35	7.01	6.8	6.93	4.96	5.55	5.4	6.73	6.67	7.31
Cr	33.9		31.4		38.6	43.3	25.8	30	32.4	34.5	27.1	30.9	11.3	28.8	23.5
Ni	30		26.3		25.7	32.3	29.3	24.7	24.3	33.7	37.7	31.6	16.2	19.9	22.6
Zn	59.8		55.9		57.7	57.6	54.7	59.3	51.7	37.2	36.7	34	49.9	49.6	49.5
As	0.501		0.304		0.364	2.59	0.646	0.362	0.373	1.39	1.1	1.85	0.417	0.614	0.744
Sb	0.077		0.036		0.070	0.043	0.097	0.071	0.082	0.175	0.223	0.287	0.050	0.092	0.179

Phenocrysts make up 32-34% of the rock and consist of 20-23% plagioclase, 7-10% hornblende, and 0.7-1.2% orthopyroxene (e.g., Table 3). Accessory minerals include apatite, ilmenite, magnetite, and pyrrhotite. Plagioclase occurs both as large sieved crystals and as smaller euhedral unsieved crystals. Plagioclase crystals have both normal and reverse zonation, with most compositions ranging between An_{40} and An_{52}. The large sieved plagioclase phenocrysts are commonly surrounded by continuous rims of zoned plagioclase. Some orthopyroxene crystals are jacketed by or complexly intergrown with hornblende. Glomerophyric clots within these lavas consist of euhedral to subhedral plagioclase, hornblende, orthopyroxene, and magnetite.

TABLE 3. Representative petrographic data for lavas of the Tschicoma Formation in the Sierra de los Valles. Phenocyst abundances are presented as a percentage of the rock.

	Dacite of Sawyer Dome	Dacite of Sawyer Dome	Dacite of Cerro Grande	Dacite of Pajarito Mt.	Dacite of Pajarito Mt.	Rhyodac. of Rendija Canyon	Rhyodac. of Rendija Canyon	Dacite of Caballo Mt.	Dacite of Caballo Mt.
Sample Number	5-25-83-1	5-25-83-4	6-22-83-3	5-5-83-1	5-13-83-1	6-24-83-1	11-83-3	8-21-88-1	8-21-88-2
Notes				lower	upper			upper	lower
Plag.	20.5	22.9	14.6	10.8	17.7	3.9	4.4	1.0	10.8
Horn.	10.0	7.0	3.0	0	0	0.2	tr	1.1	5.1
Opx	1.2	0.7	1.7	3.1	5.0	0	0	tr	tr
Cpx	0	0	0.1	1.8	1.1	0	0.1	<0.1	tr
Quartz	0	0	0	0	0	4.7	5.0	tr	1.6
Sanidine	0	0	0	0	0	0.6	4.0	0	0
Anorth.	0	0	0	0	0	0.9	1.5	0	0
Biotite	0	0	0	0	0	0.3	0.3	0	0.3
Opaques	1.6	1.1	1.0	0.8	1.4	0	0.1	nm	nm
Altered mafics	0.9	0.8	0.3	0	0	0	0.1	0	0
Total	34.2	32.5	20.7	16.5	25.2	10.6	15.5	2.1	17.8
Access-ory Min.	Ap, Mt, Ilm, Pyh	Ap, Mt, Ilm, Pyh	Ap, Mt, Ilm, Pyh	Ap, Mt, Ilm	Ap, Mt, Ilm	Sph, Mt	Zr, Sph, Mt	Ap, Mt, Ilm	Ap, Mt, Ilm
Total points	1802	1975	1866	1936	1613	1028	1566	IA	IA

IA = image analysis; tr = trace; nm = not measured. Mineral abbreviations are Plag. = plagioclase, Horn. = hornblende, Opx = orthopyroxene, Cpx = clinopyroxene, Anorth. = anorthoclase, Ap = apatite, Mt = magnetite, Ilm = ilmenite, Pyh = pyrrhotite, Sph = sphene, Zr = zircon.

Field relationships between dacites of Sawyer Dome and Cerro Grande are not known because contacts are covered by Bandelier Tuff. A sample collected at the base of the southern flank of the dome at an elevation of 9057 ft yielded an $^{40}Ar/^{39}Ar$ age of 3.67 ± 0.29 Ma (Table 4). A second sample, collected at an elevation of 9295 ft on the south flank, returned an $^{40}Ar/^{39}Ar$ age of 3.18 ± 0.20.

Dacite of Cerro Grande

The Dacite of Cerro Grande erupted as multiple lava flows from a large dome complex centered at Cerro Grande. These hornblende-rich dacites show relatively little chemical variation in major and trace elements and are compositionally distinct from the lavas of Sawyer Dome (Fig. 3; Table 2). On a volatile-free basis, these lavas contain 65.6-67.0% SiO_2, 0.57- 60% TiO_2, 4.25-4.51% Fe_2O_3T, 498-609 ppm Sr, and straddle the medium- and high- potassium fields in SiO_2 vs. K_2O plots of Le Bas et al. (1986) (Fig. 3). They also contain the lowest concentrations of uranium (1.3-1.4 ppm) and thorium (4.73-5.04 ppm) of all rocks sampled for this study (Fig. 3).

Phenocrysts make up about 21% of the rock and consist of 15% plagioclase, 3% hornblende, 1.7% orthopyroxene, and 0.1% clinopyroxene (Table 3). Accessory minerals include apatite, ilmenite, magnetite, and pyrrhotite. The lower total phenocryst content, greater orthopyroxene content, and presence of clinopyroxene clearly distinguish dacites of Cerro Grande from those of Sawyer Dome. Plagioclase occurs both as large sieved crystals and as smaller euhedral crystals. The large sieved plagioclase phenocrysts are commonly surrounded by continuous rims of complexly zoned plagioclase. Plagioclase compositions typically range between An_{44} and An_{56}. Mafic phenocrysts are relatively magnesium rich with Mg* numbers (molar Mg/(Mg+Fe)) ranging from 0.6 to 0.7 for hornblende, 0.66-0.80 for orthopyroxene, and 0.74 and 0.78 for clinopyroxene.

The Dacite of Cerro Grande is overlain by the Dacite of Pajarito Mountain on the south flank of Pajarito Mountain and in Cañon de Valle. Elsewhere contacts with other lavas are covered by Bandelier Tuff. Dalrymple et al. (1967) reported a K/Ar age of 3.67 ± 0.12 Ma for Cerro Grande lava. In this study, a sample of dacite from the north flank of Cerro Grande (elev. 9975 ft) produced an $^{40}Ar/^{39}Ar$ age of 3.07 ± 0.11 Ma and a stratigraphically lower sample from the headwaters of Cañon de Valle on the southwest flank of Pajarito Mountain (elev. 9530 ft) gave an age of 3.35 ± 0.17 Ma. Boreholes CdV-16-3(i) and CdV-R-37-2 located in the western part of the Pajarito Plateau (Fig. 1) encountered a thick stack of lavas overlain by the Puye Formation and Bandelier Tuff. The mineralogy and chemistry of the lavas in these boreholes closely match the Dacite of Cerro Grande and they appear to be correlative (Samuels et al., 2007). A sample of the dacite lava from CdV-16-3(i) yielded an $^{40}Ar/^{39}Ar$ age of 2.88 ± 0.02 Ma.

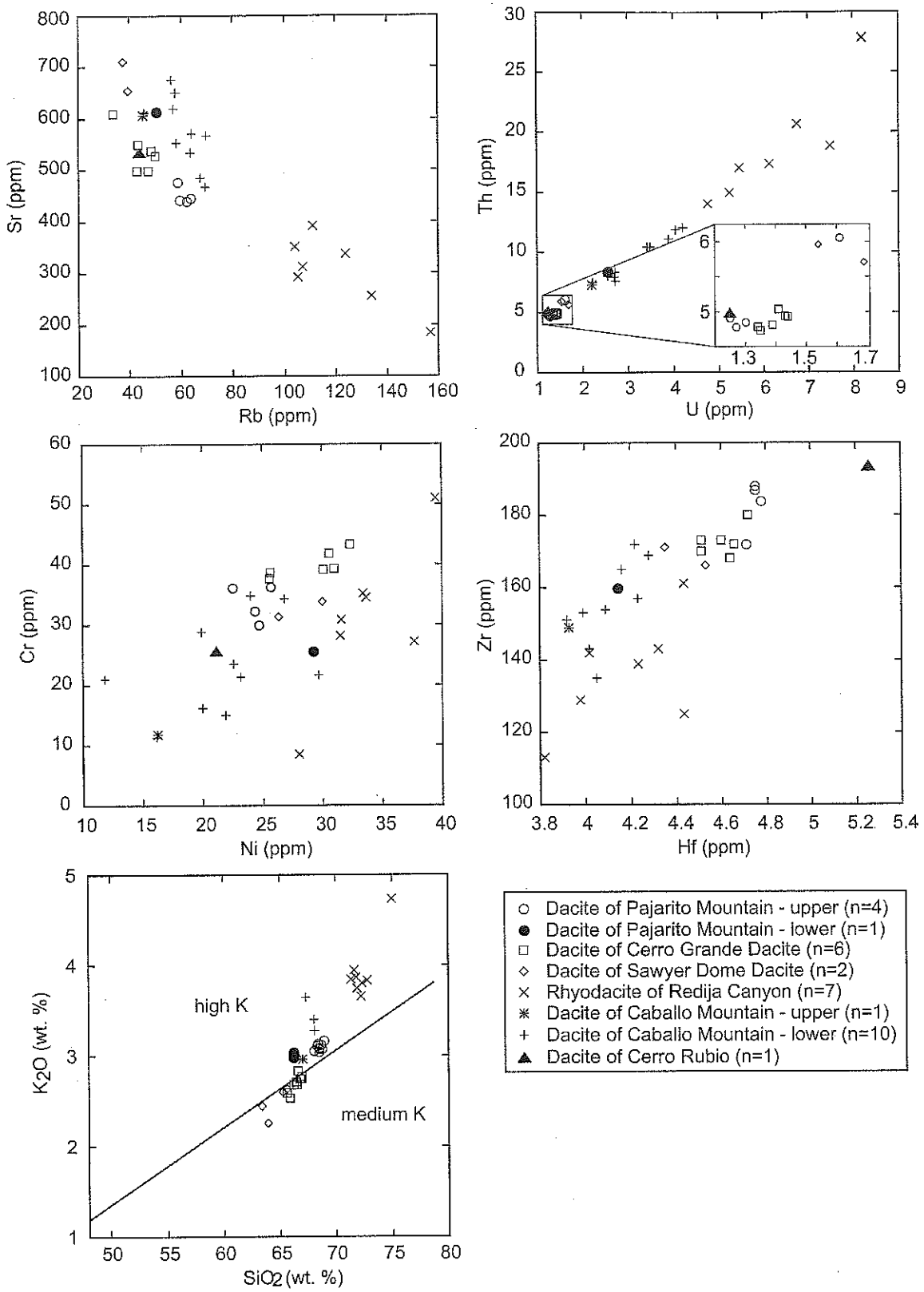

FIGURE 3. Bivariant plots showing chemical variations and relative potassium-enrichment for Tschicoma Formation from the Sierra de los Valles. The boundary between medium- and high-potassium compositions is from Le Bas et al. (1986). Analyses are plotted on a volatile-free basis. Number of samples (n) applies to top four plots based on NAA data. Number of samples for SiO_2 vs. K_2O by XRF are same as shown in Figure 2.

TABLE 4. Summary of $^{40}Ar/^{39}Ar$ Ages for Tschicoma Formation in the Sierra de los Valles and for tephras and dacite lavas in the subsurface of the Pajarito Plateau. Symbols for geologic units are: Ttsd = Dacite of Sawyer Dome, Ttcg = Dacite of Cerro Grande, Ttpm = Dacite of Pajarito Mountain; Ttcb = Dacite of Caballo Mountain; Ttrc = Rhyodacite of Rendija Canyon, Ttp = dacites in boreholes on the Pajarito Plateau, Tpa = Paliza Canyon Formation, Tpf = Puye Formation, Tb = Cerros del Rio basalt, and Qcd = Cerro Toledo dacite.

Sample	Location	Latitude NAD27	Longitude NAD27	Geologic Unit	Rock Type	Age ± 2s (Ma)
Volcanic Rocks of the Tschicoma Formation in the Sierra de los Valles						
5-25-83-1	Sawyer Dome	35.83570	106.44012	Ttsd	Andesite lava	3.67 ± 0.29
5-25-83-2	Sawyer Dome	35.83835	106.43895	Ttsd	Dacite lava	3.18 ± 0.20
6-22-83-3	Cerro Grande	35.87363	106.41076	Ttcg	Dacite lava	3.07 ± 0.11
6-22-83-5	Pajarito Mt.	35.88183	106.40814	Ttcg	Dacite lava	3.35 ± 0.17
6-22-83-9	Pajarito Mt.	35.88931	106.40261	Ttpm	Dacite lava	3.09 ± 0.08
6-22-83-12	Pajarito Mt.	35.87602	106.39933	Ttpm	Dacite lava	2.93 ± 0.06
10-8-90-2a	Pipeline Road	35.91815	106.39692	Qcd (?)	Dacite lava	1.50 ± 0.13
10-8-90-4	Pipeline Road	35.92737	106.38167	Ttcb	Dacite lava	4.66 ± 0.17
8-21-88-1	Caballo Mt.	35.95356	106.36467	Ttcb	Dacite lava	3.06 ± 0.15
LAPC98-13	North Mesa	35.89319	106.29579	Ttrc	Rhyolite lava	4.98 ± 0.05
11-19-84-1	Rendija Canyon	35.90300	106.34830	Ttrc	Rhyolite lava	5.04 ± 0.03
DEB 10-91-7	Guaje Canyon	35.86729	106.19392	Ttrc	Rhyolite tuff	5.36 ± 0.02
7-1-83-1	Los Alamos Canyon	35.88406	106.35319	Tpa	Trachyandesite lava	8.71 ± 0.10
Dacite lavas from subsurface of Pajarito Plateau						
CdV-16-3(i) at 1380-1385 ft	TA-16	35.84382	106.33187	Ttcm	Dacite lava	2.88 ± 0.02
CDV-R-15-3 at 992-997 ft	TA-16	35.84359	106.30743	Tb	Basalt lava	2.51 ± 0.09
SHB-1 at 656 ft	TA-55	35.86422	106.30477	Ttp	Dacite lava	2.36 ± 0.54
SHB-1 at 694 ft	TA-55	35.86422	106.30477	Ttp	Dacite lava	2.49 ± 0.23
R-22 at 628-638 ft	Pajarito Canyon	35.82922	106.23286	Ttp	Dacite lava	2.42 ± 0.12
Tephras from subsurface of Pajarito Plateau within Puye Formation						
R-8 at 95-95.1 ft	Los Alamos Canyon	35.87167	106.24697	Tpf	Rhyolte (?) Tephra	1.99 ± 0.05
R-25 at 1922-1923 ft	TA-16	35.84829	106.33458	Tpf	Rhyolite Tephra	5.03 ± 0.03

Dacite of Pajarito Mountain

The Dacite of Pajarito Mountain erupted as high-potassium lava flows from a dome complex centered at Pajarito Mountain. These pyroxene dacites are distinguished from the dacites of Cerro Grande by near absence of hornblende (Table 3) and slightly more evolved major and trace element chemistry (Figs. 2, 3). These lavas are divided into a lower and upper series based on differences in chemistry and mineralogy.

The lower series is a two-pyroxene dacite that crops out in Los Alamos Canyon near the Los Alamos reservoir (Fig. 1). On a volatile-free basis, these dacites are characterized by 66.6-66.7% SiO_2, 0.56-0.58% TiO_2, 4.19-4.24% Fe_2O_3T, 613 ppm Sr, 2.48 ppm U, and 8.05 ppm Th. Phenocrysts make up 10.3-16.4% of these rocks and consist of plagioclase (6.2-10.8%), orthopyroxene (2-3%), and clinopyroxene (1.5-1.8%) (Table 3). Accessory minerals include apatite and magnetite. Hornblende is present in trace amounts as alteration rims around pyroxene. Plagioclase occurs both as large sieved crystals and as smaller euhedral crystals. Glomerophyric clots (0.5%) within these lavas consist of interlocking crystals of orthopyroxene and clinopyroxene in a matrix of brown glass.

The upper series is exposed in the upper elevations of Pajarito Mountain and in upper Pajarito Canyon. On a volatile-free basis, the upper series is slightly more silicic than the lower series and contains 68.0-68.9% SiO_2, 0.47-0.49% TiO_2, 3.41-3.99% Fe_2O_3T, 441-477 ppm Sr. Despite being more silicic, the upper series contain less uranium (1.25-1.61 ppm) and thorium (4.78-6.06 ppm) than the lower series; these uranium and thorium concentrations are similar to those for dacites of Sawyer Dome and Cerro Grande. Both the upper series and lower series have chondrite-normalized rare-earth element patterns that are similar to dacites of Sawyer Dome and Cerro Grande (Fig. 4).

Phenocrysts in the upper series make up 24-25% of these rocks and consist of 17-18% plagioclase, about 5% orthopyroxene, and 1.1-1.4% clinopyroxene (Table 3). Accessory minerals include apatite, ilmenite, and magnetite. Trace hornblende is present in some samples. Plagioclase occurs both as large sieved crystals and as smaller euhedral crystals. The large sieved plagioclase phenocrysts are less abundant than in dacites of Cerro Grande. Glomerophyric clots within these lavas consist of euhedral to subhedral plagioclase and orthopyroxene ± clinopyroxene. Plagioclase compositions range between An_{30} and An_{60} with rim compositions

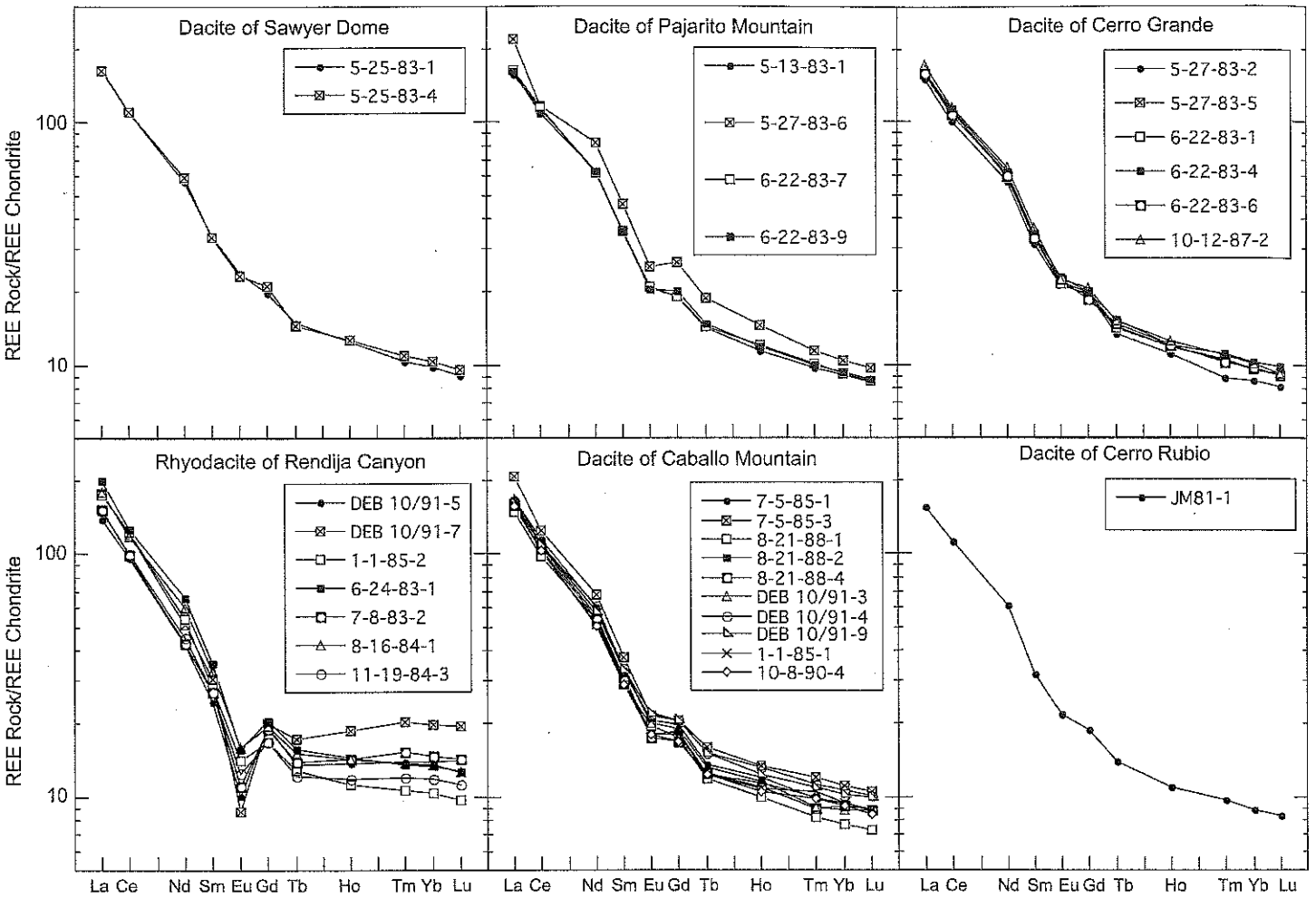

FIGURE 4. Chondrite normalized rare-earth element plots for Tschicoma volcanic rocks in the Sierra de los Valles. Rock compositions are normalized to the C1 chondrite concentrations of McDonough and Sun (1995).

clustering between An_{40} and An_{50}. Mg* ranges from 0.66-0.72 for orthopyroxene, and 0.70 and 0.78 for clinopyroxene.

Lavas of the upper series produced $^{40}Ar/^{39}Ar$ ages of 3.09 ± 0.08 Ma from a sample collected at the top of Pajarito Mountain at 10,410 ft elevation and 2.93 ± 0.06 Ma from a sample from the south flank of the mountain at 9550 ft elevation (Table 4). The lavas of the lower series have not been dated. Near the Los Alamos Canyon reservoir, the lavas of the lower series overlie an older group of lavas that include, in ascending order, trachyte, trachyandesite, and the Rhyodacite of Rendija Canyon. The trachyte (64.4 % SiO_2) and upper trachyandesite (58.7 % SiO_2) represent a small window exposing lavas of the Paliza Canyon Formation beneath the Tschicoma Formation. The trachyandesite yielded an $^{40}Ar/^{39}Ar$ age of 8.71 ± 0.10 Ma (Table 3).

Rhyodacite of Rendija Canyon

The Rhyodacite of Rendija Canyon is a voluminous stack of lavas and minor tuffs erupted from a dome complex located in the headwaters of Rendija Canyon. One particularly large lobe of lava flowed down the east flank of the dome complex and across the western part of the Española basin to Guaje Mountain (Fig. 1). The Rendija Canyon dome complex is so deeply eroded that the original volcanic structure is unrecognizable. Gardner et al. (2006) described a possible vent high on a ridge north of the headwaters of Quemazon Canyon.

Although named the Rhyodacite of Rendija Canyon, silica and alkali compositions for samples from this unit fall within the rhyolite field in the classification of La Bas et al. (1986) (Fig. 2). Small-volume high-silica lavas and tuffs exposed in western Guaje Canyon are believed to represent an early eruptive phase of Rendija Canyon volcanism. Low-silica rhyolites constituting the main part of the Rendija Canyon lavas contain 71.4-72.8% SiO_2, 0.29-0.39% TiO_2, 2.32-3.02% Fe_2O_3T, and 293-392 ppm Sr, on a volatile-free basis. Concentrations of uranium (4.76-6.75 ppm) and thorium (14-20.7 ppm) are significantly greater than the other lavas of the Tschicoma Formation. Chondrite-normalized rare-earth element patterns display conspicuous negative europium anomalies (Fig. 4). A single sample of high-silica rhyolite lava in Guaje Canyon has a volatile-free composition of 75.1% SiO_2, 0.21% TiO_2, and 1.46% Fe_2O_3T. NAA results for two high-silica rhyolite samples yielded 7.49-8.2 ppm U, 18.8-27.8 ppm Th, and 183-255 ppm Sr.

Phenocrysts make up 11-16% of the low-silica rhyolites and consist of quartz (4.7-5%), plagioclase (3.9-4.4%), sanidine (0.6-4%), and anorthoclase (0.9-1.5%). Mafic phenocrysts generally make up <0.5% of these rocks and consist of biotite ± clinopyroxene ± hornblende (Table 3). Accessory minerals include magnetite and zircon ± sphene. Quartz is commonly resorbed and plagioclase and anorthocase are typically strongly sieved. The groundmass includes felty plagioclase, acicular orthopyroxene, and clinopyroxene. Plagioclase compositions typically range between An_{28} and An_{12}, and overlap into the anorthoclase compositional field. In one sample, euhedral microphenocrysts of plagioclase are unusually calcic, with compositions ranging between An_{30} and An_{50}. Sanidine compositions range between Or_{54} and Or_{62}. Mg* numbers in mafic phenocrysts are 0.60-0.64 for biotite, 0.72 to 0.80 for clinopyroxene, and 0.76-0.86 for groundmass orthopyroxene. Modal data are not available for the high-silica rhyolite, but phenocrysts consist of quartz, sanidine, plagioclase, and anorthoclase (?) with subordinate biotite, rare clinopyroxene and hornblende, and accessory magnetite and sphene.

A sample of Rendija Canyon rhyolite from upper Rendija Canyon yielded a K/Ar age of 4.55 ± 0.22 Ma (F.W. McDowell, personal commun., 1987). In this study, a sample of the low-silica rhyolite from North Mesa in Los Alamos produced an $^{40}Ar/^{39}Ar$ age of 4.98 ± 0.05 Ma and a sample from the headwaters of Rendija Canyon yielded an age of 5.04 ± 0.03 Ma (Table 4). A sample from a small ash-flow tuff collected in Guaje Canyon 1.8 km upstream of the reservoir returned an $^{40}Ar/^{39}Ar$ age of 5.36 ± 0.02 Ma.

Dacite of Caballo Mountain

Caballo Mountain is a large volcanic dome that was the source of voluminous high-potassium dacite flows that produced major flow lobes directed towards the east (Kempter and Kelley, 2002). On a volatile-free basis, these lavas contain 65.6-68.5% SiO_2, 0.49-0.55% TiO_2, 3.42-4.21% Fe_2O_3T, 468-570 ppm Sr. Most major and trace elements for these lavas are similar to those found in the dacites of Sawyer Dome, Cerro Grande, and Pajarito Mountain. However, dacites of Caballo Mountain differ from these other dacites by a greater range in trace element compositions and by higher concentrations of uranium (2.55-4.05 ppm) and thorium (7.98-11.8 ppm) (Fig. 3).

Petrographic characteristics also vary greatly. Rocks at the summit of Caballo Mountain contain about 2% phenocrysts consisting of subequal plagioclase and hornblende, subordinate clinopyroxene, and trace quartz and orthopyroxene. These relatively crystal-poor lavas overlie crystal-rich lavas on the northeast, east, and south flanks of Caballo Mountain. The major-element chemistry of the crystal-poor and crystal-rich dacites is similar, but the trace element data indicate the upper crystal-poor dacites are slightly less evolved than the lower lavas (Table 2). The most crystal-rich lavas form the ridgeline at about 9700 ft elevation northeast of Caballo Mountain; phenocrysts in these lavas make up approximately 24% of the rock and consist of plagioclase (~19%), hornblende (~3%), sanidine (~1%) quartz (~0.5%), and biotite (~0.2%). Orthopyroxene and clinopyroxene are present in trace amounts. Lavas exposed to the south and east of Caballo Mountain contain about 12-19% phenocrysts consisting predominantly of plagioclase and hornblende with subordinate amounts of quartz and biotite. Orthopyroxene and clinopyroxene are present in trace amounts. All these lavas contain plagioclase that occurs both as large sieved and wormy phenocrysts and as smaller euhedral phenocrysts. A diverse collection of glomerophyric clots are present in these lavas, including clots composed of plagioclase, hornblende, hornblende-plagioclase, plagioclase-hornblende-biotite, hornblende-biotite, and clinopyroxene-orthopyroxene.

The dacites of Caballo Mountain overlie the Rhyodacite of Rendija Canyon on the south flank of Caballo Mountain and on the ridgeline in the northwest headwaters of Quemazon Canyon. The stratigraphic relationship between the Dacite of Caballo Mountain and dacite lavas to the north at Tschicoma Mountain are unknown. A sample of dacite with ~2% phenocrysts from the summit of Caballo Mountain yielded an$^{40}Ar/^{39}Ar$ age of 3.06 ± 0.15 Ma (Table 4). A sample of crystal-rich Caballo dacite from the ridgeline above Quemazon Canyon returned an $^{40}Ar/^{39}Ar$ age of 4.66 ± 0.17 Ma. The age difference between these lavas is much greater than for other domes where more than one age date was obtained. Both dates appear to be free of significant analytical error, and they are consistent with the stratigraphic positions of these lavas. The greater range of trace element compositions, variable phenocryst contents, and range of $^{40}Ar/^{39}Ar$ ages indicate that eruptions at Caballo Mountain spanned a longer time period and represent a wider variety of lavas than eruptions from other dome complexes.

DISCUSSION

Lavas of the Tschicoma Formation within the central and southern Sierra de los Valles erupted from overlapping dome and flow complexes between about 5.3 and 2.9 Ma. These ages fall within the range of previously reported dates for the Tschicoma Formation throughout the Jemez volcanic field (Dalrymple et al., 1967; Luedke and Smith, 1978; Gardner et al., 1986; Goff and Gardner, 2004).

There are limited spatial or temporal trends in eruption sequence or magma compositions among the dome complexes. The oldest lavas (Rhyodacite of Rendija Canyon) are the most silicic. Individual volcanic centers show an evolution in magma compositions over time. For example, the Rhyodacite of Rendija Canyon apparently became less silicic as the eruptions proceeded. The least silicic lavas (Sawyer Dome) were erupted during the middle part of the 2.5 m.y. period of eruptions of the Tschicoma Formation in this area; these hornblende dacites became more silicic as eruptions from this dome complex proceeded. One of the youngest dome complexes (Pajarito Mountain) is composed of rocks intermediate in composition between the Rendija Canyon and Sawyer Dome lavas; these lavas also became slightly more silicic during the course of their eruption.

Lavas of the Tschicoma Formation are medium- to high-potassium dacites and rhyolites. One interesting feature of these lavas is the very low concentrations of uranium and thorium in the dacites of Sawyer Dome, Cerro Grande, upper series Pajarito

Mountain, and Cerro Rubio. These rocks contain between 1.25 and 1.69 ppm uranium and 4.73 and 6.06 ppm thorium. Such low concentrations for these incompatible elements indicate derivation from relatively mafic source rocks and minimal fractionation prior to eruption. The Rhyodacite of Rendija Canyon is the only unit containing a negative Eu anomaly indicative of feldspar fractionation. The dacite lavas lack conspicuous Eu anomalies and generally have closely overlapping rare-earth element patterns, with the exception of dacites of Caballo Mountain, which show a range of compositions that mirror their range in modal mineralogy (Table 3). Lack of conspicuous Eu anomalies in dacites of the Tschicoma Formation is somewhat surprising because all of them are plagioclase phyric. The plagioclase in these rocks includes both highly sieved megacrysts up to 5 mm in size and unsieved microphenocrysts about 0.2-0.8 mm in size. Extensive sieving and resorption textures indicate the plagioclase megacrysts were not in equilibrium with their magmas. Although megacrysts commonly occur as single crystals, many consist of glomerophyric clusters of plagioclase ± other minerals. The megacrysts may represent varying stages of disaggregation of glomerophyic clots. Lack of a Eu anomaly in the Tschicoma dacites may reflect the accumulation of plagioclase megacrysts by these magmas that masks evidence of feldspar fractionation by the host magma. Alternatively, these magmas may have erupted before significant fractionation took place, as suggested by the U and Th data.

The rare-earth and other trace element compositions in the Dacite of Caballo Mountain are more variable than the other dacites in this study. Their variable compositions may reflect in part accumulation of varying amounts of plagioclase, hornblende, quartz, and biotite megacrysts that are particularly abundant in these rocks (cf. the two examples in Table 3). At Caballo Mountain, the crystal-poor lavas have the lowest content of U, Th, and REE. Like plagioclase, the hornblende, quartz, and biotite megacrysts show evidence of disequilibrium (resorption of quartz, jacketing of biotite by hornblende) and they too may represent disaggregated glomerophyic clots. Although it seems likely the megacrysts and glomerocrysts in these rocks are cognate, their disequilibrium textures suggest they formed under different temperature, pressure, or chemical conditions than those that prevailed in their host lavas prior to eruption.

One unexpected result from the $^{40}Ar/^{39}Ar$ dates is a 1.50 ± 0.13 Ma age obtained for a dacite lava exposed along Pipeline Road on the ridge forming the western headwaters of Quemazon Canyon. This lava is relatively crystal poor (<5% phenocrysts) and contains plagioclase, clinopyroxene, and orthopyroxene phenocrysts. The 1.50 Ma age suggests this lava is part of the Cerro Toledo Rhyolite, a collection of high-silica rhyolite flow and dome complexes clustered within the Toledo embayment about 4 km to the northwest. Cerro Toledo rhyolites range in age from 1.21± 0.01 to 1.65 ± 0.03 Ma (Heiken et al., 1986; Spell et al., 1996). Because known exposures of the Cerro Toledo consist entirely of rhyolite, the dacitic composition of this lava is unusual. The $^{40}Ar/^{39}Ar$ result on a groundmass concentrate has good analytical precision, and there are no obvious analytical problems with the reported age. Nonetheless, because of its unusual composition, a new sample was collected and will be dated to provide additional control for the age of this dacite (F. Goff, personal commun., 2005).

Two samples were collected for age determinations from pumice falls intercalated within the Puye Formation in boreholes on the Pajarito Plateau. In borehole R-8 (Fig. 1), pumices collected at a depth interval of 95-95.1 ft yielded an $^{40}Ar/^{39}Ar$ date of 1.99 ± 0.05 Ma. This sample was collected near the top of the Puye Formation in a 27 m-thick sequence of brown silts and fine sands that contain abundant biotite-bearing pumice. This portion of the Puye Formation overlies Cerros del Rio basalt, establishing an upper limit for the age of these basalts at this location. Attempts to date tephras in borehole R-8 within the lower part of the Puye Formation beneath the Cerros del Rio basalt resulted in ages with poor confidence that are not reported. In borehole R-25 (Fig. 1), pumices collected at a depth of 1922-1923 ft yielded a $^{40}Ar/^{39}Ar$ date of 5.03 ± 0.03. These pumices are rhyolitic and probably represent a primary Rendija Canyon fall deposit interbedded with proximal alluvial fan deposits containing cobbles and boulders of Rhyodacite of Rendija Canyon. The age of the pumice deposit and compositions of clasts within the alluvial fan indicate that volcanism, erosion, and sediment deposition was synchronous during this time. Also, the great thickness of Puye Formation in this borehole (>330 m) suggests that significant subsidence took place in the western Española basin since at least 5 Ma to accommodate the massive influx of sediment derived from erosion of the Tschicoma Formation.

Small-volume dacites that occur in several boreholes on the Pajarito Plateau were also dated by $^{40}Ar/^{39}Ar$ methods. A companion paper by Samuels et al. (2007) describes the distribution, chemistry, and petrography of these dacites. The sample from borehole CdV-16-3(i) yielded an age of 2.88 ± 0.02 Ma and is the oldest of the borehole dacites (Table 4). As discussed previously, the CdV-16-3(i) dacite is believed to be correlative with the Dacite of Cerro Grande. Other dacites beneath the Pajarito Plateau erupted between 2.36 ± 0.54 and 2.49 ± 0.23 Ma, postdating Tschicoma volcanism in the Sierra de los Valles. These relatively young ages overlap with those for the Cerros del Rio basalts (WoldeGabriel et al., 2001). However, the chemistry of these dacites is more closely allied to the Tschicoma Formation. Apparently, voluminous silicic to intermediate volcanism took place over a period of about 2.5 m.y. in the central and southern Sierra de los Valles before dying out at approximately 2.9 Ma. Volcanism then shifted southeastwards across the western Española basin where small-volume dacites and the basalts of the Cerros del Rio volcanic field were erupted.

ACKNOWLEDGMENTS

We thank our reviewers David Vaniman and Richard Warren for their constructive comments that greatly improved the paper. Our ideas about the geology of the Tschicoma Formation have greatly benefited from discussions and field excursions with our colleagues, especially Rick Warren, David Vaniman, Jamie Gardner, Fraser Goff, Kirt Kempter, and Shari Kelley. Rick Warren and Frank Byers provided some of the samples used in this study.

Steve Bolivar and Larry Maassen accompanied the lead author on several very enjoyable sample collection trips.

REFERENCES

Bailey, R.A., Smith, R.L., and Ross. C.S. 1969, Stratigraphic nomenclature of volcanic rocks in the Jemez Mountains, New Mexico: U.S. Geological Survey, Bulletin 1274-P, 19 p.

Broxton, D., Warren, R., Longmire, P., Gilkeson, R., Johnson, S., Rogers, D., Stone, W., Newman, B., Everett, M., Vaniman, D., McLin, S., Skalski, J., and Larssen, D., 2002, Characterization well R-25 completion report: Los Alamos National Laboratory, Report LA-13909-MS, 77 p.

Broxton, D.E., WoldeGabriel, G., Peters, L., Budahn, J., and Luedemann, G., 2007, $^{40}Ar/^{39}Ar$ data repository for Pliocene volcanic rocks of the Tschicoma Formation, east-central Jemez volcanic field: chemistry petrography, and age constraints: New Mexico Bureau of Geology and Mineral Resources, Open File Report OF-AR-30, 30 p.

Budahn, J.R. and Wandless, G.A., 2002, Instrumental neutron activation analysis by long count, *in* Taggert, E. Jr., ed., Analytical methods for chemical analysis of geologic and other materials: U.S. Geological Survey, Open File Report 02-0223, Chapter X.

Criss, J., 1979, Criss Software Inc., 12204 Blaketon St., Largo, MD 20870.

Dalrymple, G.B., Cox, A., Doell, R.R., and Grommé, C.S., 1967, Pliocene geomagnetic polarity epochs: Earth and Planetary Science Letters, v. 2, p. 163-173.

Gardner, J.N., Goff, F., Garcia, S., and Hagan, R.C., 1986. Stratigraphic relations and lithologic variations in the Jemez volcanic field, New Mexico: Journal of Geophysical Research, v. 91, p. 1763-1778.

Gardner, J.N., Goff, F., Reneau, S.L., Sandoval, M.M., Drakos, P.G., Katzman, D., and Goff, C.J., 2006, Preliminary geologic map of the Valle Toledo 7.5-minute quadrangle, Los Alamos and Sandoval Counties, New Mexico: New Mexico Bureau of Geology and Mineral Resources, Open-file Geologic Map OF-GM 133, scale 1:24,000.

Goff, F., and Gardner, J.N., 2004, Late Cenozoic geochronology of volcanism and mineralization in the Jemez Mountains and Valles caldera, north central New Mexico, *in* Mack, G.H., and Giles, K.A., eds., The geology of New Mexico, a geologic history: New Mexico Geological Society, Special Publication 11, p. 295-312.

Goff, F., Gardner, J., Baldridge, W. S., Hulen, J., Nielson, D., Vaniman, D., Heiken, G., Dungan, M., and Broxton, D., 1989, Volcanic and hydrothermal evolution of Valles caldera and Jemez volcanic field: Field Excursion 17B: New Mexico Bureau of Mines and Mineral Resources, Memoir 46, p. 381-434.

Goff, F., Reneau, S.L., Lynch, S., Goff, C.J., Gardner, J.N., Drakos, P., and Katzman, D., 2005, Preliminary geologic map of the Bland 7.5-minute quadrangle, Los Alamos and Sandoval Counties, New Mexico: New Mexico Bureau of Geology and Mineral Resources, Open-file Geologic Map OF-GM-112, scale 1:24,000.

Griggs, R.L., 1964, Geology and ground-water resources of the Los Alamos area, New Mexico: U.S. Geological Survey, Water Supply Paper 1753, 107 p.

Heiken, G., Goff, F., Stix, J., Tamanyu, T., Shafiqullah, M, Garcia, S., and Hagan, R., 1986, Intracaldera volcanic activity, Toledo caldera and embayment, Jemez Mountains, New Mexico: Journal of Geophysical Research, v. 91, p. 1799-1815.

Kempter, K.A. and Kelley, S., 2002, Preliminary geologic map of Guaje Mountain 7.5-minute quadrangle, Los Alamos and Sandoval Counties, New Mexico: New Mexico Bureau of Geology and Mineral Resources, Open-file Geologic Map OF-GM 55, scale 1:24,000.

Le Bas, M. J., Le Maitre, R. W., Streckeisen, A., and Zanettin, B., 1986, A chemical classification of volcanic rocks based on the total alkali-silica diagram: Journal of Petrology, v. 27, p. 745-750.

Luedke, R.G., and Smith. R.L., 1978, Map showing distribution, composition, and age of late Cenozoic volcanic centers in Arizona and New Mexico: U.S. Geological Survey, Miscellaneous Geological Investigation Map I-1091-A, scale 1:1,000,000.

McDonough, W.F., and Sun, S., 1995, Composition of the Earth: Chemical Geology, v. 120, p. 223-253.

McIntosh, W. C., and Cather, S. M., 1994, $^{40}Ar/^{39}Ar$ geochronology of basaltic rocks and constraints on late Cenozoic stratigraphy and landscape development in the Red Hill-Quemado area, New Mexico: New Mexico Geological Society, 45th Field Conference, Guidebook, p. 209-224.

Samson S.D., and Alexander, E.C. Jr., 1987, Calibration of the interlaboratory ^{40}Ar-^{39}Ar dating standard MMhb-1: Chemical Geology (Isotope Geoscience), v. 66, p. 27–34.

Samuels, K.E., Broxton, D.E., Vaniman, D.T., WoldeGabriel, G., Wolff, J.A., Hickmott, D.D., Kluk, E.C., Fittipaldo, M.M., 2007, Distribution of dacite lavas beneath the Pajarito Plateau, Jemez Mountains, NM: New Mexico Geological Society, 58th Field Conference, Guidebook, p.296-307.

Smith, H.T.U., 1938, Tertiary geology of the Abiquiu quadrangle, New Mexico: Journal of Geology, v. 46, p. 933-965.

Smith, R.L., Bailey, R.A., and, Ross C.S, 1970. Geologic map of the Jemez Mountains, New Mexico: U.S. Geological Survey, Miscellaneous Geological Investigation Map I-571, scale 1:125,000.

Spell, T.L., McDougall, I., and Doulgeris, A.P., 1996, Cerro Toledo Rhyolite, Jemez volcanic field, New Mexico: $^{40}Ar/^{39}Ar$ geochronology of eruptions between two caldera-forming events: Geological Society of America Bulletin, v. 108, p.1549–1566.

Turbeville, B.N., Waresback, D.B., and Self, S., 1989, Lava dome growth and explosive volcanism in the Jemez Mountains, New Mexico – evidence from the Pliocene-Pleistocene Puye alluvial fan: Journal of Volcanology and Geothermal Research, v. 36, p. 267-291.

Waresback, D.B., and Turbeville, B.N., 1990, Evolution of a Pliocene-Pleistocene volcanogenic alluvial fan – the Puye Formation, Jemez Mountains, New Mexico: Geological Society of America Bulletin, v. 102, p. 298-314.

Warren, R.G., Cole, G.L., Broxton, D.E., Kluk, E.C., Chipera, S.J., WoldeGabriel, G., Vaniman, D.T., Snow, M.G., and Goff, F., 2005, A database of geochemical, petrographic, mineralogic, and geochronological analyses for the Jemez volcanic field to support the 3-D geologic model of the Pajarito Plateau, Los Alamos National Laboratory, New Mexico: Los Alamos National Laboratory, Unlimited Release LA-UR-05-2976.

WoldeGabriel, G., Warren, R.G., Broxton, D.E., Vaniman, D.T., Heizler, M.T., Kluk, E. C., and Peters, L., 2001, Episodic volcanism, petrology, and lithostratigraphy of the Pajarito Plateau and adjacent areas of the Española Basin and the Jemez Mountains: New Mexico Museum of Natural History and Science, Bulletin 18, p. 97-129.